

Classical Physics and Blackbody Radiation

Jiao Wang,^{1,2} Giulio Casati,^{3,4} and Giuliano Benenti^{3,5,6}

¹*Department of Physics and Key Laboratory of Low Dimensional Condensed Matter Physics (Department of Education of Fujian Province), Xiamen University, Xiamen 361005, Fujian, China*

²*Lanzhou Center for Theoretical Physics, Lanzhou University, Lanzhou 730000, Gansu, China*

³*Center for Nonlinear and Complex Systems, Dipartimento di Scienza e Alta Tecnologia, Università degli Studi dell'Insubria, via Valleggio 11, 22100 Como, Italy*

⁴*International Institute of Physics, Federal University of Rio Grande do Norte, Campus Universitário - Lagoa Nova, CP. 1613, Natal, Rio Grande Do Norte 59078-970, Brazil*

⁵*Istituto Nazionale di Fisica Nucleare, Sezione di Milano, via Celoria 16, 20133 Milano, Italy*

⁶*NEST, Istituto Nanoscienze-CNR, I-56126 Pisa, Italy*

We investigate the properties of the blackbody spectrum by direct numerical solution of the classical equations of motion of a one-dimensional model that contains the essential general features of the field-matter interaction. Our results, which do not rely on any statistical assumption, show that the classical blackbody spectrum exhibits remarkable properties: (i) a quasistationary state characterized by scaling properties, (ii) consistency with the Stefan-Boltzmann law, and (iii) a high-frequency cutoff. Our work is a preliminary step in the understanding of statistical properties of infinite dimensional systems.

Introduction.— The inability of classical physics to account for the experimentally observed frequency spectrum of blackbody radiation is at the origin of quantum theory. In spite of desperate attempts, the falloff of the blackbody curve at high frequencies could not be explained by classical mechanics. To be more precise, however, this is not a failure of classical theory *per se*. Indeed, it is the classical theory with the additional assumption of energy equipartition which leads to the Rayleigh-Jeans radiation law, implying the unphysical ultraviolet catastrophe [1].

On the other hand, classical ergodic theory, from which equipartition theorem follows, is valid only for systems with a *finite* number of degree of freedoms. Ergodicity, that is, independence of time averages on initial conditions, does not imply equipartition of energy for a system with infinite degrees of freedom, since there is no invariant measure at hand to define a microcanonical ensemble. A main difficulty here stems from the fact that the radiation field has $N_m = \infty$ degrees of freedom (modes) and that the two limits $N_m \rightarrow \infty$ and time $t \rightarrow \infty$ do not commute. Therefore, the question of what classical mechanics predicts on the properties of the radiation field in equilibrium with matter is still open.

Even more interesting is the Stefan-Boltzmann law which states that at temperature T the total radiation energy $E \propto T^4$. It is remarkable that this formula, which is well in agreement with experimental data, was derived by Boltzmann in 1884 on *purely classical thermodynamics basis* [2]. As such, it should be a consequence of the classical equations of motion. Notice that this result is formally in contradiction with the Rayleigh-Jeans law, according to which $E \propto T$.

What about the solution of the nonlinear classical Newton-Maxwell equations of motion that govern the field-matter interaction? Will dynamics agree and to

what extent, with the above classical statistical and thermodynamics predictions? After 150 years, this question concerning a fundamental problem in the development of modern physics remains unsolved.

Here, we numerically integrate the exact classical equations of motion of a blackbody model, without any statistical assumption, and we show that classical dynamics leads to a quasistationary state that is consistent with the Stefan-Boltzmann law and where the energy distribution over the field normal modes exhibits an exponentially decreasing tail. Therefore the solution of the classical equations of motion naturally leads to a high-frequency cutoff of the blackbody spectrum.

Model.— To investigate the dynamics of charged particles interacting with the electromagnetic field in a cavity is a formidable task. Here we consider a variant of a model introduced long ago [3] and afterwards studied in several papers [4–10]. In spite of its simplicity, our model retains the general essential features of field-matter interaction: (i) the field modes can only exchange energy via interaction with matter and (ii) the free electromagnetic field in the cavity is by itself a linear system and nonlinearity is provided by matter.

A sketch of our model is drawn in Fig. 1. It consists of an electromagnetic field confined in between two parallel, perfectly reflecting plane mirrors, a distance $2l$ apart. We take Cartesian coordinates xyz with the x axis normal to the mirrors and restrict to excitations only dependent on x , thus getting a one-dimensional radiant cavity, the normal modes of which have angular frequencies ω_k . We then introduce N_p coupled plates, which are all parallel to the mirrors and which are constrained to move only in the z direction. Only the plate positioned midway between the mirrors is charged and therefore interacts with the normal modes of the field. We denote by σ and m the charge and mass densities per unit surface of the plate,

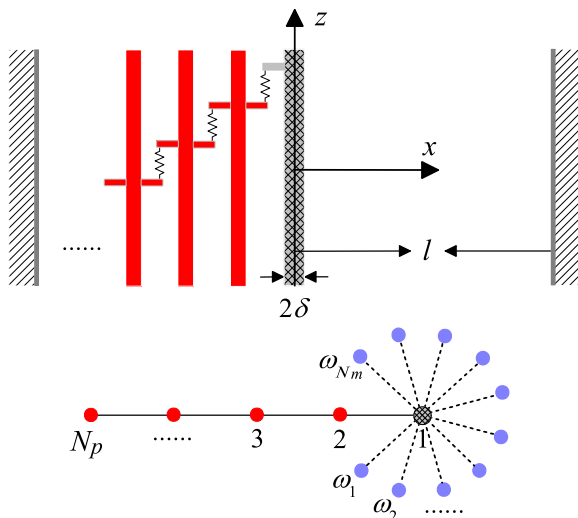


FIG. 1: Schematic drawing (top) of the classical radiant cavity model. A charged plate of width 2δ is placed at the center of the cavity bounded by two mirrors a distance $2l$ apart. The charged plate interacts with a fixed number of neutral plates (to the left in the figure) and with the normal modes of the electromagnetic field. The topology of interactions is also shown (bottom), where the gray dot, red dots, and blue dots are for the charged plate, the neutral plates, and the field modes, respectively.

and $f(x)$ is the normalized (transverse) distribution of charge in the plate, whose thickness is 2δ .

The Hamiltonian of the full system, plates plus field, can be written as

$$H = \sum_{j=2}^{N_p} \left[\frac{P_j^2}{2m} + \tilde{V}(z_j) + V(z_{j-1}, z_j) \right] + \tilde{V}(z_1) + \frac{1}{2m} (P_1 - \varepsilon \sum_{k=1}^{\infty} a_k q_k)^2 + \frac{1}{2} \sum_{k=1}^{\infty} (p_k^2 + \omega_k^2 q_k^2), \quad (1)$$

where P_j and z_j are the conjugate momentum and displacement of the j th plate, \tilde{V} and V are the on site and interacting potentials of plates, and p_k and q_k are conjugate variables of the k th normal mode of the field with frequency ω_k . Note that the field normal modes are infinite but, as we shall see below, only a finite, small number $N_m(t)$ of them are actually involved during the computation time. In Eq. (1), the term $\frac{1}{2m} (P_1 - \varepsilon \sum_{k=1}^{\infty} a_k q_k)^2$ accounts for the interaction between the charged plate and the normal modes, where $\varepsilon = 2\sigma\sqrt{\pi/l}$ is the matter-field coupling parameter. We assume that $f(x)$ is an even function, and therefore, even normal modes do not interact with the charged plate, while for an odd normal mode with wave number $2k-1$, $a_k = \int_{-\delta}^{\delta} f(x) \cos \frac{\omega_k x}{c} dx$, where c is the speed of light and $\omega_k = \frac{\pi c}{2l}(2k-1)$.

If the charge is removed, $\varepsilon = 0$, the plates and the modes are decoupled. We choose, as interaction potential among the matter degrees of freedom, the lattice ϕ^4

model [11, 12]

$$\tilde{V}(z_j) = \frac{1}{4} \gamma z_j^4, \quad V(z_{j-1}, z_j) = \frac{1}{2} \kappa (z_j - z_{j-1})^2. \quad (2)$$

We checked that, for $N_p > 4$ and for an average energy per plate larger than 0.1 (in our units $l = \pi$, $c = m = \sigma = 1$, and the Boltzmann constant $k_B = 1$; moreover we set $\gamma = \kappa = 1$), this model is chaotic with N_p positive Lyapunov exponents.

Initially, all the energy is assigned to matter only (the plates), and we focus on how the energy is transferred and distributed among the field normal modes. For the charge distribution we choose $f(x) = A \exp(\frac{\delta^2}{x^2 - \delta^2})$ ($|x| < \delta$) (a compactly supported C^∞ function, with A normalization constant, $A = 45.04\dots$ for the width $\delta = 0.05$ used in our simulations). We have verified that, qualitatively, the results do not depend on the particular choice of the charge distribution, provided it is a smooth function (see Supplemental Material [13]). In addition, we take $N_p = 16$ and we have verified that the whole system remains chaotic during the entire relaxation process accessible to simulations ($t \sim 10^9$) [13].

Results.— Since our simulations are for energies well above the stochasticity threshold, for any *finite* number of field modes, equipartition is expected among the degrees of freedom. Our first step is therefore to investigate how long it takes for equipartition to set in. As shown in Fig. 2, equipartition is reached among the plates after a relatively short time, τ_p , that, basically, does not depend on the number N_m of field modes. Instead, global equipartition among field and matter degrees of freedom is reached after a time τ_m that exponentially increases with N_m . The best fitting suggests $\tau_m \sim e^{1.29 N_m}$, in clear contrast with $\tau_p \approx 10^3$ [13]. If we extrapolate this exponential dependence of the equipartition time τ_m to larger N_m values, then it turns out that already for $N_m \approx 48$ field normal modes, a time of the order of the age of the Universe is required in order to reach equipartition (in a cavity of $l \sim 1$ m). Note that the two limits $t \rightarrow \infty$ and $N_m \rightarrow \infty$ do not commute. If one takes the limit $t \rightarrow \infty$ first, then one will always get equipartition while for the blackbody problem it is necessary to take the limit $N_m \rightarrow \infty$ first. In order to simulate this latter situation, in our computations we take $N_m = 120$, which, in view of the results of Fig. 2, is sufficiently large to neglect the higher normal modes.

We now turn to the energy distribution over the field normal modes. In Fig. 3(a) we plot the average energy $\langle E_{m,k}(t) \rangle$ of the normal modes over their frequency. The main feature of the distribution $\langle E_{m,k} \rangle$ is the presence of a plateau followed by a rapid, exponential decay. The average value $\langle E_{m,k} \rangle$ of the plateau normal mode energies is equal to the average energy $\langle E_{p,j} \rangle$ of the plates. This suggests that the field modes in the plateau are thermalized with matter, at temperature $T = \langle E_{p,j} \rangle$. This thermalization process evolves in time very slowly; indeed, as

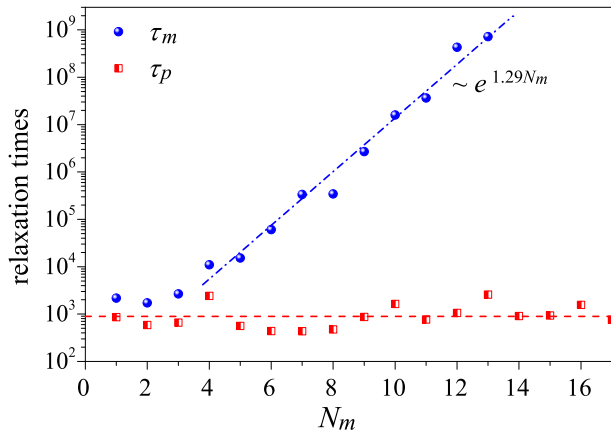


FIG. 2: The relaxation time of plates (τ_p) and of both plates and field modes (τ_m), where N_m field modes are considered in the simulation. Here the number of plates $N_p = 16$, and the total energy $E_{tot} = 2^4$ is initially assigned to the charged plate as kinetic energy. For other initial conditions where the total energy is distributed randomly among the plates, $\tau_m \sim e^{1.29 N_m}$ still holds.

seen in Fig. 3(a), it takes about 3 orders of magnitude in time (from 10^5 to 10^8) in order to increase only by four the number of thermalized modes. This observation is consistent with the results of Fig. 2 and suggests that the system relaxes to a quasistationary state after which it evolves very slowly, logarithmically in time.

It is remarkable that the quasistationary state has a clear scaling property. This is shown in Figs. 3(b) and 3(c), where we plot $\langle E_{m,k}(t) \rangle / T(t)$ over $[\omega_k - \alpha \ln(t)]$ and over $\beta[\omega_k - \alpha \ln(t)]$, where α and β depend on the total energy only, $\alpha = 0.23 E_{tot}^{0.24}$ and $\beta = 3.22 E_{tot}^{-0.22}$ based on the best fitting of the data for $10^4 \leq t \leq 10^8$ and $2^4 \leq E_{tot} \leq 2^{10}$.

We cannot give a rigorous explanation for the appearance of an exponential cutoff. Nevertheless, we can provide an intuitive understanding by observing (see Fig. 4) that, as is typically the case for nonlinear interacting systems, the power spectrum of the charged plate has a finite frequency band, followed by an exponential tail. For the field modes within this band, thermalization with matter is achieved rapidly. On the other hand, for the field modes with frequencies in the exponential tail, thermalization requires exponentially long timescales. We can see from Fig. 4 that the power spectrum is, in practice, independent of the number N_p of plates (for a fixed energy per plate), while for a given N_p the bandwidth increases with the total energy E_{tot} . Such dependence is consistent with the reduction of the thermalization times (up to a given frequency) with increasing E_{tot} .

Note that the total energy of the modes in the exponential tail is negligible compared with that of the thermalized modes on the plateau. Therefore, it is tempting to conjecture that the quasistationary state should be

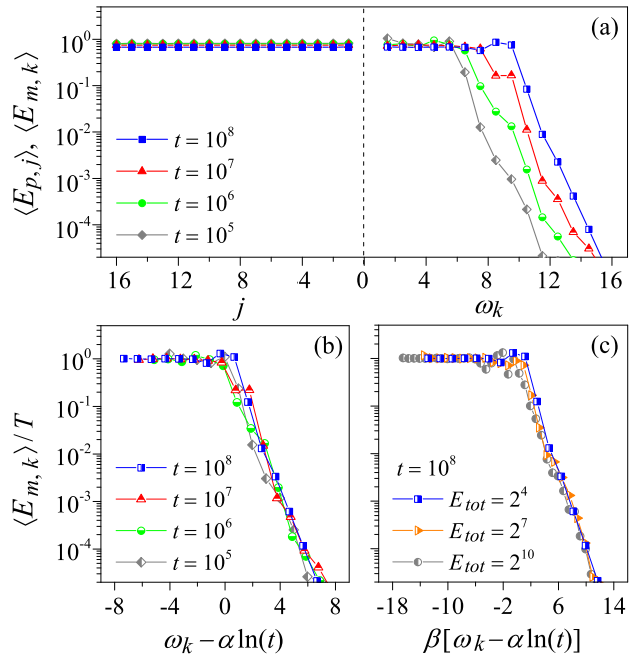


FIG. 3: (a) The average energy of the plates (full symbols) and of the field modes (half filled symbols), for total energy $E_{tot} = 2^4$ at different times. (b) $\langle E_{m,k} \rangle$ scaled by the temperature of plates and the mode frequencies being shifted by $\alpha \ln(t)$. (c) $\langle E_{m,k} \rangle$ versus the scaled and shifted frequencies at a given time. The results for different total energies collapse on the same curve. The energy of the system is initially randomly assigned to the plates as kinetic energy.

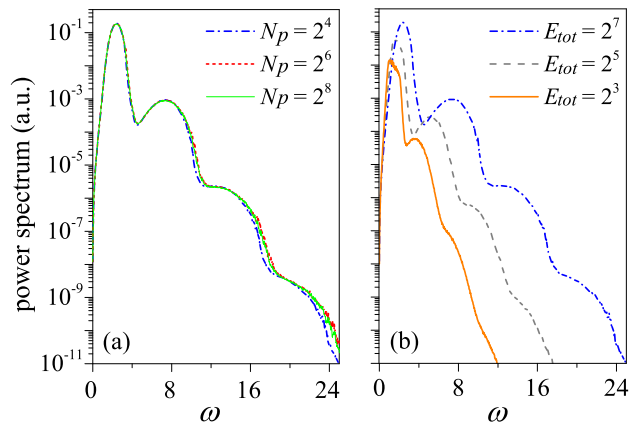


FIG. 4: Power spectrum of the time series $P_1(t)$ for the momentum of the charged plate, in a system of N_p plates with total energy E_{tot} , for (a) $E_{tot}/N_p = 8$ and (b) $N_p = 16$.

approximately described by equilibrium thermodynamics. To this end, following Boltzmann, we start from the fundamental thermodynamic relation $dU = TdS - pdV$,

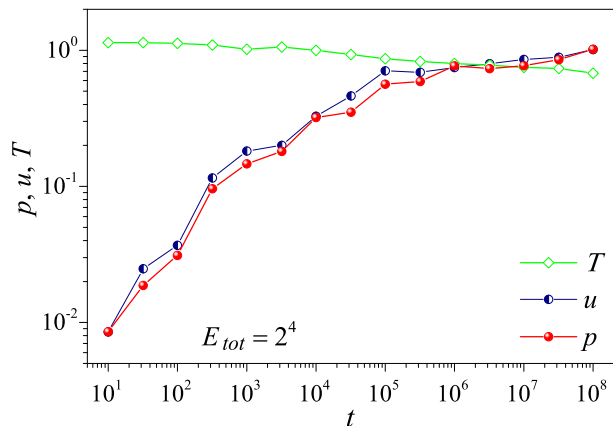


FIG. 5: The pressure p , the energy density u of the cavity, and the temperature T of the plates as functions of time.

which implies

$$\left. \frac{\partial U}{\partial V} \right|_T = -p + T \left. \frac{\partial p}{\partial T} \right|_V, \quad (3)$$

where $U = U(T, V)$ is the total energy, S is the entropy, p is the pressure of the radiation field, V is the volume of the cavity, and T is the temperature of the plates. The relation between the energy of the electromagnetic radiation and its pressure has been derived by Boltzmann and for the one-dimensional case reads:

$$p = u, \quad (4)$$

where $u = U/V$ is a universal function of temperature and independent of volume. From Eq. (3) one then has

$$u(T) = CT^2, \quad (5)$$

where C is a constant. This is the Stefan-Boltzmann law in one dimension. Quite remarkably, these predictions based on equilibrium thermodynamics are consistent with our model in the quasistationary state. In Fig. 5, we plot p , u , and T versus the evolution time for $E_{tot} = 2^4$. Here p is numerically computed [13] and $T = \langle E_{p,j} \rangle$ is the temperature of matter. It can be noticed that the relation (4) between energy density and pressure sets in almost immediately. In Fig. 6, we plot u versus T for various values of the total energy of the system. It is seen that $u \propto T^B$ where the exponent $B(t)$ increases from 1.07 to 1.21, as time t goes from 10^4 to 10^8 . This dependence is compatible with Eq. (5). Indeed the inset of Fig. 6 suggests that the value 2 might be approached logarithmically in time.

Summary and discussion.— In summary, we have studied a model of a classical radiant cavity. If one considers a fixed, finite number N_m of field modes, then the system, as expected, approaches equipartition, even though the

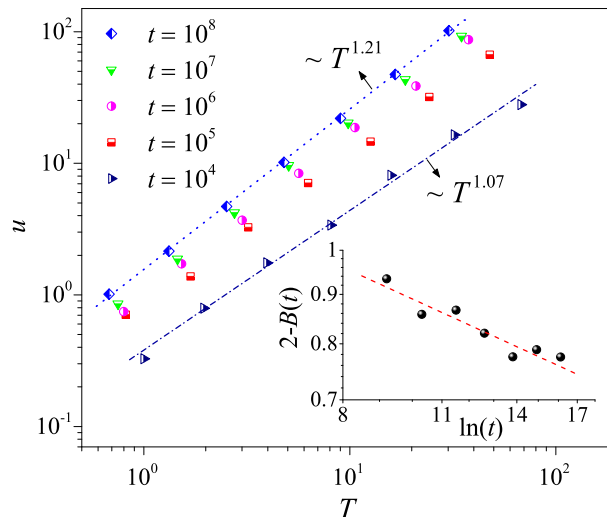


FIG. 6: The energy density u in the cavity versus the temperature T of the plates at various evolution times. At a given time, the seven data points correspond to total energies $E_{tot} = 2^4, 2^5, \dots, 2^{10}$, respectively. At each time the data exhibit a power law relation $u \propto T^B$, and the best fitting shows that the power law exponent $B(t)$ slowly changes from 1.07 to 1.21 as time changes by 4 orders of magnitude. The fitting line in the inset gives the expression $2 - B(t) \sim (\ln t)^{-0.33}$.

relaxation times increase exponentially with the number N_m of modes. If instead one takes the limit $N_m \rightarrow \infty$ first, as it is required in order to study the blackbody radiation, then the system relaxes to a quasistationary state characterized by a low frequency plateau, followed by a high frequency exponential cutoff. The computed field energy density turns out to be consistent with the Stefan-Boltzmann law.

Our model contains the basic ingredients of an electromagnetic field interacting with matter. Since interaction among the field modes is mediated by mechanical degrees of freedom, in general, we expect thermalization of the field modes with matter to be effective only within the frequency bandwidth of mechanical motion, with slow thermalization outside such bandwidth. We therefore conjecture that the appearance of a time-dependent cutoff is a general feature of classical dynamics of matter-field interaction. Nevertheless, it would be interesting to investigate higher-dimensional models or, more generally, other classical field theories. Such studies could help our understanding of the statistical properties of nonlinear dynamical systems with infinite degrees of freedom. In this frame, the results presented here on a classical model can be considered a preliminary step before addressing ergodicity in quantum field theories. This problem will require a nontrivial extension of concepts and tools recently developed for the investigation of thermalization and localization in many-body quantum systems [14–18].

We acknowledge support by the NSFC (Grants No.

12075198 and No. 12047501) and by the INFN through the project QUANTUM.

SUPPLEMENTAL MATERIAL

Results for other charge distributions

In this section, we show that the exponentially slow relaxation of the field modes is a general feature, independent of the particular charge distribution $f(x)$. For this purpose we focus, in between the other charge distributions we have considered (apart from the one in the main text), on two limiting cases: the Dirac delta function and the hump function. The Dirac-delta function $f(x) = \delta(x)$ is an extreme case, for which the coefficients a_k are constant. On the other hand, for smooth functions like the hump function $f(x) = B(\delta^2 - x^2)/(\delta^4 + x^4)$ or the function $f(x) = A \exp(\delta^2/(x^2 - \delta^2))$ considered in the main text, (for both functions, with a numerical normalization factor in front) the coefficients a_k decay with k faster than algebraically (see Fig. 7).

Below we report the results for the relaxation time and the average energy of the plates and of the field modes, corresponding to Figs. 2 and 3(a) of the main text, but for the delta and the hump function. While for the hump charge distribution the obtained results are quite similar to those reported in the main text (see Fig. 8), for the delta-function distribution the energy transfer to the field modes is more efficient (see Fig. 9). On the other hand, it appears clearly that also in this limiting case the average energy of the normal modes drops exponentially after the thermalization plateau and before the algebraic tail $\propto 1/k^2$ determined by the coefficients a_k (see below). The exponential decay goes down to smaller and smaller energy as time increases and more normal modes are thermalized. Moreover, thermalization of the field modes is again logarithmically slow in time, the relaxation time for N_m normal modes being $\tau_m \sim e^{\alpha N_m}$, even though the coefficient $\alpha = 0.54$ is smaller than the value $\alpha = 1.29$ obtained for the smooth functions (the hump distribution and the distribution considered in the main text).

Finally, we add the explanation of the power-law tail observed in Fig. 9(b). For that purpose, it is enough to consider the linear model with the charged plate coupled to the cavity modes. That is, the second line of Eq. (1) of the main text:

$$H_{\text{lin}} = \frac{1}{2m}(P_1 - \varepsilon \sum_{k=1}^{\infty} a_k q_k)^2 + \frac{1}{2} \sum_{k=1}^{\infty} (p_k^2 + \omega_k^2 q_k^2). \quad (6)$$

In this case, the state of the system at time t , written as an ∞ -dimensional vector,

$$\mathbf{q}(t) = \left\{ m^{1/2} \dot{z}_1(t), \dots, \omega_k q_k(t), p_k(t), \dots \right\}, \quad (7)$$

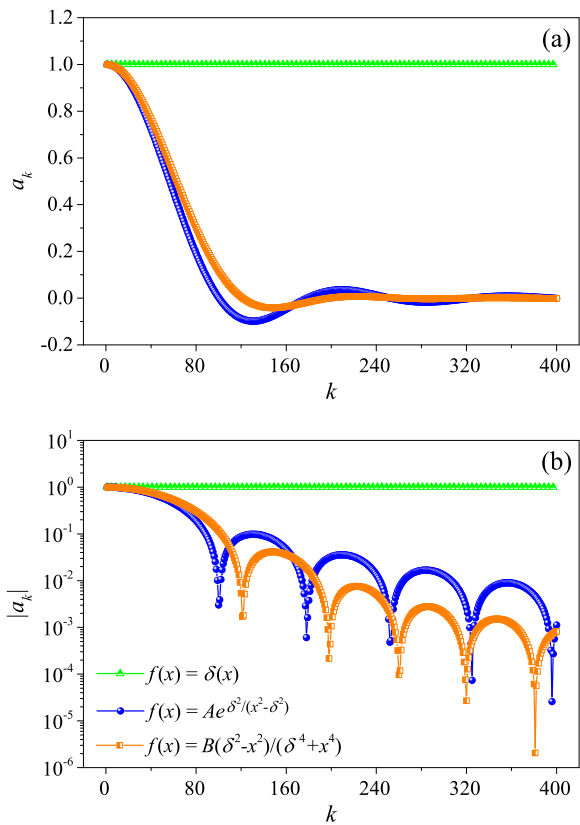


FIG. 7: Coupling coefficients a_k (top panel) between the charged plate and the k -th field mode, and their absolute values $|a_k|$ (bottom panel), for three charge distribution functions considered in our study. The coefficients corresponding to $f(x) = A \exp(\frac{\delta^2}{x^2 - \delta^2})$ and $f(x) = B \frac{\delta^2 - x^2}{\delta^4 + x^4}$ (in both cases, $\delta = 0.05$, and correspondingly $A = ???$ and $B = ???$) oscillate around zero and meanwhile decay, while for the Dirac delta function $a_k = 1$, independently of k .

(the total energy is the square norm of such vector) can be expanded over the eigenstates of the overall (plate plus cavity) linear system,

$$\mathbf{u}_k = C_k \left\{ 1, \dots, \frac{\varepsilon a_k \omega_k}{\Omega_k^2 + \omega_k^2}, \frac{\varepsilon a_k \Omega_k}{\Omega_k^2 + \omega_k^2}, \dots \right\}, \quad (8)$$

where $\varepsilon = 2\sigma(\pi/ml)^{1/2}$ and C_k is a normalization constant. These eigenvectors define normal modes of the total system, with eigenfrequencies Ω_k given by the imaginary roots of the secular equation:

$$\Omega_k \left(1 + \varepsilon^2 \sum_{n=1}^{\infty} \frac{a_n^2}{\Omega_k^2 + \omega_n^2} \right) = 0. \quad (9)$$

In the linear system, there is no thermalization and the field modes are populated as determined by the Fourier coefficients a_k . In particular, for large k , the energy on mode k drops as $1/k^2$ when the charge distribution $f(x)$ is a Dirac delta-function ($a_k = 1$ independently of k in

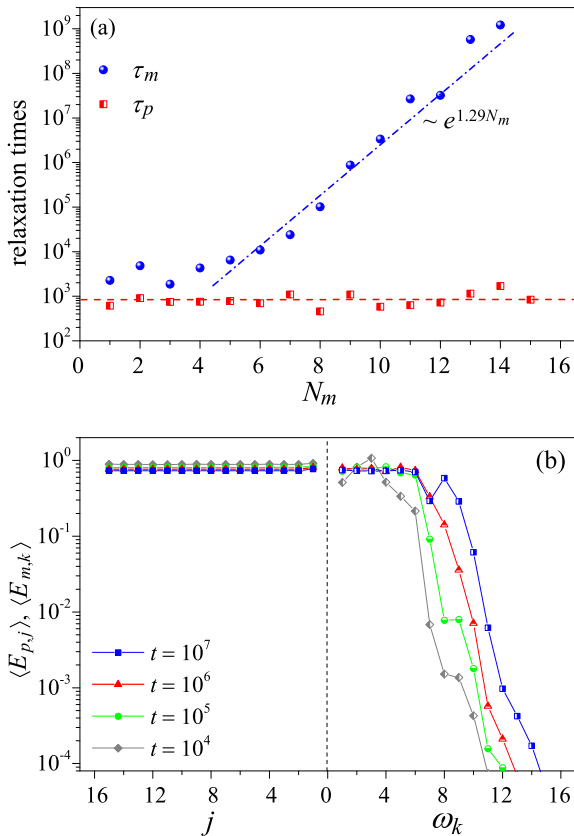


FIG. 8: The relaxation process for the case where the charge distribution function is a smooth function, $f(x) = B(\delta^2 - x^2)/(\delta^2 + x^4)$, with $\delta = 0.05$ and $B = 19.51\dots$ (a) Relaxation time of plates (τ_p) and of both plates and field modes (τ_m). (b) Average energy of the plates (full symbols) and of the field modes (half-filled symbols) at different times, for total energy $E_{tot} = 16$.

this case), and faster than algebraically for the hump distribution and the distribution considered in the main text.

On the other hand, such difference does not affect qualitatively the conclusions of our study when nonlinear terms, mixing the normal modes, are added, inducing exponentially slow thermalization of the field modes, independently of the particular choice of $f(x)$.

Details of numerical simulations

In our numerics, we have used a 4th order Runge-Kutta algorithm, with integration time step $\Delta t = 10^{-4}$, which we have verified to be short enough to ensure reliable results up to $t \sim 10^9$ and for total energy E_{tot} ranging between 16 and 1024.

We have defined the energies $E_{m,k} = p_k^2$ and $E_{p,j} = P_j^2$. In order to suppress fluctuations, we perform, for a given initial condition, a partial time average of $E_{m,k}(t)$

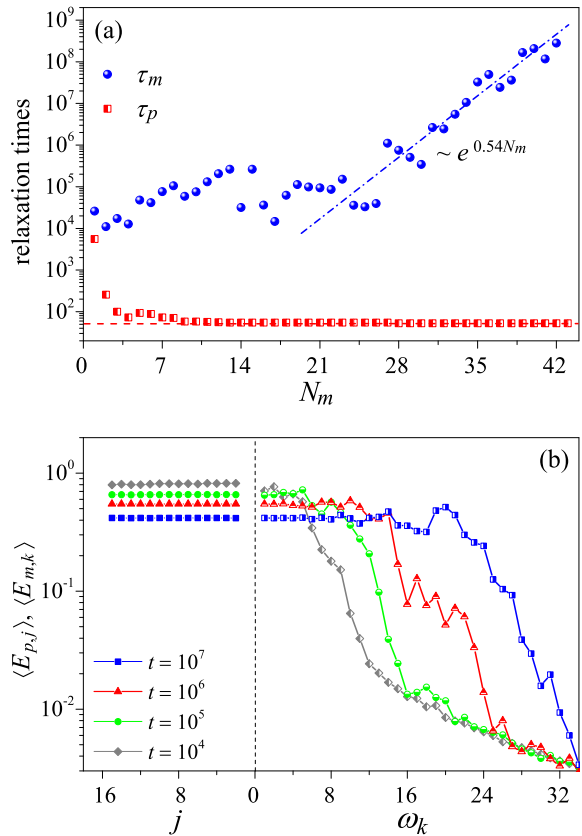


FIG. 9: As in Fig. 8, but for the limiting case where the charge distribution function is a Dirac δ -function, $f(x) = \delta(x)$.

over the time interval $(t, 2t)$. In addition we make an ensemble average (denoted as $\langle \dots \rangle$) over nine initial conditions. For the normal modes of the field, we have checked that $\langle p_k^2 \rangle = \omega_k^2 \langle q_k^2 \rangle$. For the neutral plates, using the equipartition theorem we obtain

$$\left\langle P_j \frac{\partial H}{\partial P_j} \right\rangle = \left\langle z_j \frac{\partial H}{\partial z_j} \right\rangle, \quad (10)$$

that is, using $\langle z_j z_k \rangle = 0$ for $j \neq k$,

$$\langle P_j^2 \rangle = \langle 2\tilde{V}(z_j) + V(z_{j-1}, z_j) + V(z_j, z_{j+1}) \rangle. \quad (11)$$

We have checked numerically this latter equation.

In order to evaluate the equipartition times τ_p and τ_m , we have adopted the equipartition indicator given in Ref. [10]. Namely, we compute $S_p(t) = \sum_{j=1}^{N_p} \overline{E}_{p,j}(t) \ln \overline{E}_{p,j}(t)$ and $S_m(t) = \sum_{k=1}^{N_m} \overline{E}_{m,k}(t) \ln \overline{E}_{m,k}(t)$, where $\overline{E}_{p,j}(t)$ and $\overline{E}_{m,k}(t)$ are the time averages of P_j^2 and p_k^2 up to time t , respectively. Then the value $\exp[-S_p(t)]$ is a measure of the number of plates significantly excited up to time t . We thus define τ_p as the time at which this value reaches 90% of N_p . The same procedure is used to define τ_m .

To measure numerically the pressure at a given time, a perturbation of $-2\Delta l$ to the distance between the two

mirrors is imposed; the pressure is identified to be the ratio of the responding ΔE_{tot} over $2\Delta l$.

The fortran codes involved in this study are available. Those who are interested, please contact the authors.

-
- [1] F.R.S. Lord Rayleigh, *Philos. Mag.* **49**, 539 (1900); J. H. Jeans, *The dynamical Theory of Gases*, 4th ed. (Cambridge University Press, Cambridge, England, 2009).
- [2] L. Boltzmann, *Ann. Phys. (Berlin)* **258**, 291 (1884); *Nature (London)* **51**, 413 (1895).
- [3] P. Bocchieri, A. Crotti, and A. Loinger, *Lett. Nuovo Cimento* **4**, 741 (1972).
- [4] P. Bocchieri, A. Loinger, and F. Valz-Gris, *Nuovo Cimento B* **19**, 1 (1974).
- [5] G. Casati, I. Guarneri, and F. Valz-Gris, *Phys. Rev. A* **16**, 1237 (1977).
- [6] G. Benettin and L. Galgani, *J. Stat. Phys.* **27**, 153 (1982).
- [7] G. Casati, I. Guarneri, and F. Valz-Gris, *J. Stat. Phys.* **30**, 195 (1983).
- [8] R. Livi, M. Pettini, S. Ruffo, and A. Vulpiani, *J. Phys. A* **20**, 577 (1987).
- [9] C. Alabiso, M. Casartelli, and S. Sello, *J. Stat. Phys.* **54**, 361 (1989).
- [10] G. Benenti, G. Casati, and I. Guarneri, *Europhys. Lett.* **46**, 307 (1999).
- [11] K. Aoki and D. Kusnezov, *Phys. Lett. A* **265**, 250 (2000).
- [12] G. Parisi, *Europhys. Lett.* **40**, 357 (1997).
- [13] See supplemental material, where Ref. [10] is included, for results obtained for other charge distributions and details on numerical simulations.
- [14] A. Polkovnikov, K. Sengupta, A. Silva, and M. Vengalattore, *Rev. Mod. Phys.* **83**, 863 (2011).
- [15] R. Nandkishore and D. A. Huse, *Annu. Rev. Condens. Matter Phys.* **6**, 15 (2015).
- [16] F. Borgonovi, F. M. Izrailev, L. F. Santos, and V. G. Zelevinsky, *Phys. Rep.* **626**, 1 (2016).
- [17] L. D'Alessio, Y. Kafri, A. Polkovnikov, and M. Rigol, *Adv. Phys.* **65**, 239 (2016).
- [18] D. A. Abanin, E. Altman, I. Bloch, and M. Serbyn, *Rev. Mod. Phys.* **91**, 021001 (2019).